

PACS numbers: 42.70.Qs, 61.05.cp, 73.20.Mf, 78.20.Ci, 78.40.Kc, 78.67.Bf, 81.07.Wx

## Investigations on the Linear Optical Properties of Copper, Silver and Gold Nanoparticles for Surface-Plasmon Resonance Applications

R. Salome Mercy Ponrani<sup>1</sup>, S. G. Rejith<sup>1</sup>, D. Esther Nancy<sup>2</sup>,  
and S. C. Vella Durai<sup>3</sup>

<sup>1</sup>*Department of Physics, St. Xavier's College,  
Palayamkottai,  
IN-627002 Tirunelveli, Tamil Nadu, India*

<sup>2</sup>*Department of Physics, Sarah Tucker College,  
IN-627007 Tirunelveli, Tamil Nadu, India*

<sup>3</sup>*PG and Research Department of Physics, Sri Paramakalyani College,  
Alwarkurichi,  
IN-627412 Tenkasi, Tamil Nadu, India*

Noble metals have been extensively studied for plasmonic energy, catalysis, photonics, and sensing applications because of their high localized surface-plasmon resonance (LSPR) responses. The LSPR phenomenon, which is the collective oscillation of electrons on metallic nanoparticles (NPs) triggered by light photons at the resonant frequency. This property is present in metal NPs like Au, Ag, and Cu. Using power x-ray diffraction (PXRD) method, structural analysis is carried out. Diffuse reflectance spectroscopy (DRS) of UV-Vis is a predominantly helpful method for describing the LSPR behaviour of metallic NPs. In this work, chemical reduction method is used to fabricate gold, silver, and copper NPs, and UV DRS is used to examine their LSPR activity (there is a plasmon-resonance peak for pure copper, silver, and gold NPs).

Шляхетні метали були широко вивчені для застосувань у плазмонній енергетиці, каталізі, фотоніці та сенсориці завдяки їхній високій чутливості щодо локалізованого поверхневого плазмонного резонансу (ЛППР). Явище ЛППР — це колективне коливання електронів на металевих наночастинках (НЧ), що викликається фотонами світла на резонансній частоті. Ця властивість присутня в металевих НЧ, таких як Au, Ag і Cu. За допомогою методу дифракції потужних Рентгенових променів (ДПП) проводиться структурна аналіза. Дифузна відбивна спектроскопія (ДВС) УФ- й видимого діяпазону є переважно корисним методом для опису поведінки ЛППР металевих НЧ. У цій роботі для виготовлення НЧ золота, срібла та міді використано метод хемічного відновлення, а ДВС УФ-діяпазону — для дослідження їхньої ЛППР-

активності (є пік плазмонного резонансу для чистих НЧ Cu, Ag та Au).

**Key words:** nanoparticles, resonance, LSPR, spectroscopy, DRS.

**Ключові слова:** наночастинки, локалізований поверхневий плазмонний резонанс, дифузна відбивна спектроскопія.

*(Received 10 November, 2024)*

## 1. INTRODUCTION

Noble metals have attracted a lot of attention just now because of their exceptional performance in a range of catalytic processes and their numerous uses. In addition to their diverse electrical, chemical, optical, and magnetic characteristics, noble metal nanoparticles (NPs) reveal strong catalytic capabilities [1–3]. Because of their nanometer-scale size and shape, metallic NPs have gained lot of interest. Absorption, transmission, reflection, and light emission are only a few of the dynamic optical features of NPs, which set them apart from bulk materials [4].

Surface-plasmon resonance and optical properties are two of the exceptional qualities of metallic NPs. Metal NPs are utilized in optical biosensor applications due to their surface-plasmon resonance (SPR) feature [5]. Gold, silver, copper, lead, and platinum NPs' optical characteristics are caused by the resonant oscillation of their free electrons in the presence of light, which is sometimes referred to as localized surface-plasmon resonance (LSPR) [6].

Laser photothermal treatment for cancer uses this SPR absorption in NPs. The optical characteristics of metal NPs are essential for a number of applications, including imaging sensors, displays, solar cells, photocatalysis, biomedicine, optical detectors, and lasers [7]. A number of variables, including metal composition, shape, and particle size, affect the LSPR peaks.

This work examines the linear optical characteristics of powdered copper, silver, and gold NPs, which have undergone chemical reduction. Powder x-ray diffraction is used to confirm the structure, and UV-Vis DRS is used to inspect the linear optical behaviour.

## 2. MATERIALS AND METHODS

### 2.1. Preparation of NPs

In this study, copper, silver, and gold NPs are synthesized using the chemical reduction approach. Here, nitrate salts of copper and silver serve as precursors, while ethanol is utilized as a stabilizer



Fig. 1. Synthesized (a) copper NPs, (b) silver NPs, (c) gold NPs.

along with sodium borohydride and hydrazine hydrate as reducing agents. The chemicals used are of analytical grade. In the preparation of pure silver NPs, 0.1 M of hydrazine hydrate and 0.1 M of sodium borohydride solution were added drop by drop to an aqueous solution of  $\text{AgNO}_3$  (0.5 M) that was being continuously agitated by a magnetic stirrer. The reduction of metal nitrate to metal is confirmed by the colour shift from transparent solution to dark grey. To stabilize the process at that point, 1 ml of ethanol was added. Centrifugation was used to remove the precipitate from the solution by subsequent three hours of constant stirring. The synthesized materials were thoroughly cleaned with ethanol and then dried in a hot air oven at  $100^\circ\text{C}$  for three hours. A closed vial was used to collect the dried material. The same method is used for preparing pure copper NPs; here,  $\text{Cu}(\text{NO}_3)_2$  is taken as a precursor.

In the preparation of pure gold NPs, 0.001 M of gold chloride solution, 0.1 M of sodium borohydride, and 0.1 M of hydrazine hydrate are combined and agitated in drops on a magnetic stirrer for three hours at a speed of roughly 500 revolutions per minute. Ascorbic acid (0.2 g) is then added. The reduction of metal NPs is indicated by the colour shift. To stabilize the process, ethanol is now added. The precipitate is separated from the solution after stirring. After being cleaned with ethanol, the synthesized material is heated to  $100^\circ\text{C}$  for approximately two hours in a hot air oven. A closed vial is used to collect the prepared sample. The synthesized NPs are shown in Fig. 1.

## 2.2. Characterization Techniques

Power x-ray diffraction (PXRD) method is one of the analytical tools simply used to study the crystallographic structure of the sample. Further, it helps to recognize the phase and purity of the

sample along with the structural parameters. With specialized refinement techniques, it ensures straightforward data interpretations. In this study, the instrument Bruker D8 advance is used to take the x-ray diffractogram of the sample Ag, Au, and Cu NPs. The surface-plasmon resonance behaviour of the synthesized NPs is studied by analysing the diffuse reflectance spectrum, which is a useful tool for studying the spectral characteristics of opaque solid samples by the specular and diffuse reflections of light. The UV-DRS spectrum was recorded in the Shimadzu UV-2600PC series.

### 3. RESULTS AND DISCUSSION

#### 3.1. Powder X-Ray Diffraction Analysis

The powder x-ray diffraction patterns of Cu, Ag, and Au NPs are shown in Fig. 2. In these diffractograms, the presence of a series of

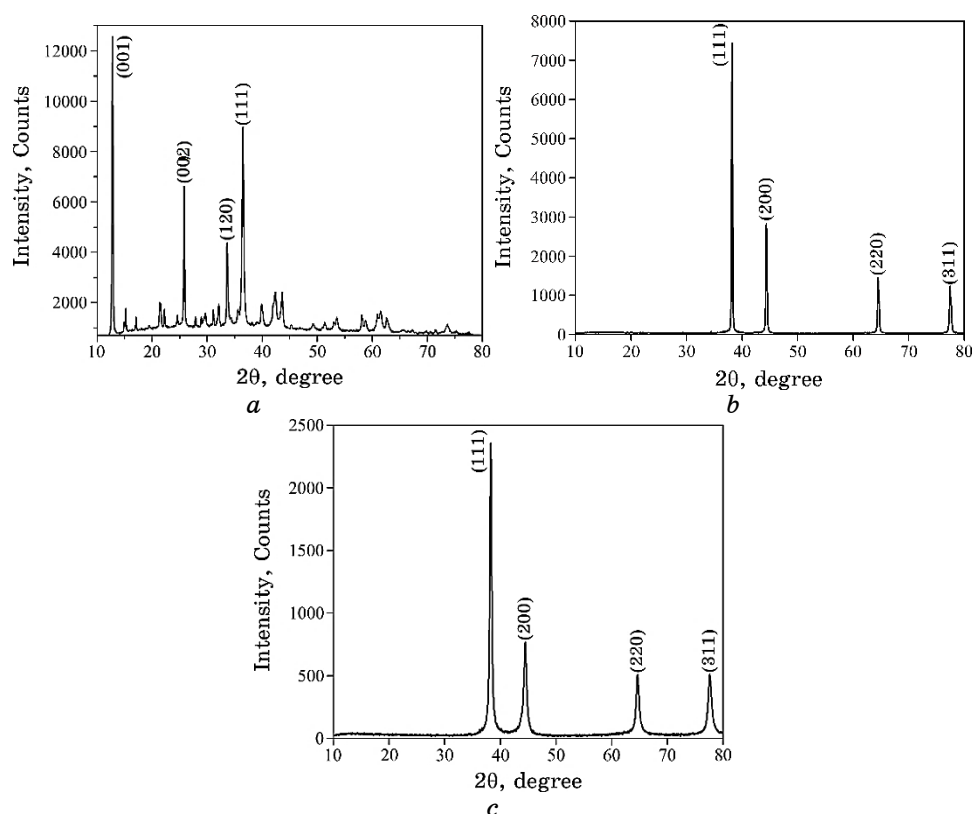


Fig. 2. PXRD pattern of (a) Cu NPs, (b) Ag NPs, (c) Au NPs.

**TABLE 1.** The crystalline structural details of the Cu, Ag and Au NPs.

No.	NPs	ICDD (JCPDS) Card No.	Crystal structure	Lattice constant
1	Cu	04-0836	f.c.c.	$a = 3.614 \text{ \AA}$
2	Ag	04-0783	f.c.c.	$a = 4.086 \text{ \AA}$
3	Au	04-0784	f.c.c.	$a = 4.0786 \text{ \AA}$

**TABLE 2.** Crystallite size of the Cu, Ag, and Au NPs.

No.	NPs	Average crystallite size
1	Cu	40.62 nm
2	Ag	35.91 nm
3	Au	18.59 nm

sharp and well-defined reflection peaks at periodic intervals is evident that the synthesized NPs have a high degree of crystallinity [8]. The diffractogram has been compared with the standard powder diffraction card of the ICDD (JCPDS) file and indexed. All the three synthesized metal NPs are belonging to the face-centred cubic structure. The crystallographic details of Cu, Ag, and Au NPs are given in Table 1.

In the x-ray diffraction pattern, (111), (200), (220), and (311) are the prominent reflection planes, which are observed in all three diffractograms [9–11]. These reflections are in agreement with those reported in previous works.

Utilizing powder x-ray diffraction (PXRD), the average crystallite size ( $D$ ) of the NPs was estimated from the diffractogram using the Scherrer formula:

$$D = \frac{0.9\lambda}{\beta \cos \theta} .$$

The calculated crystallite sizes are summarized in Table 2, indicating that all values fall within the nanometer range.

### 3.2. Diffuse Reflectance Spectral Analysis

Noble metals, including copper, silver, and gold NPs, exhibit unique optical properties, which enable strong interactions with specific wavelengths of light. Their distinct absorption spectra in the UV and visible regions arise from the collective oscillation of free electrons, resonating with incident light waves [12].

Metals typically exhibit highly reflective surfaces. In the context of UV DRS, both surface reflectance and diffuse reflectance of the

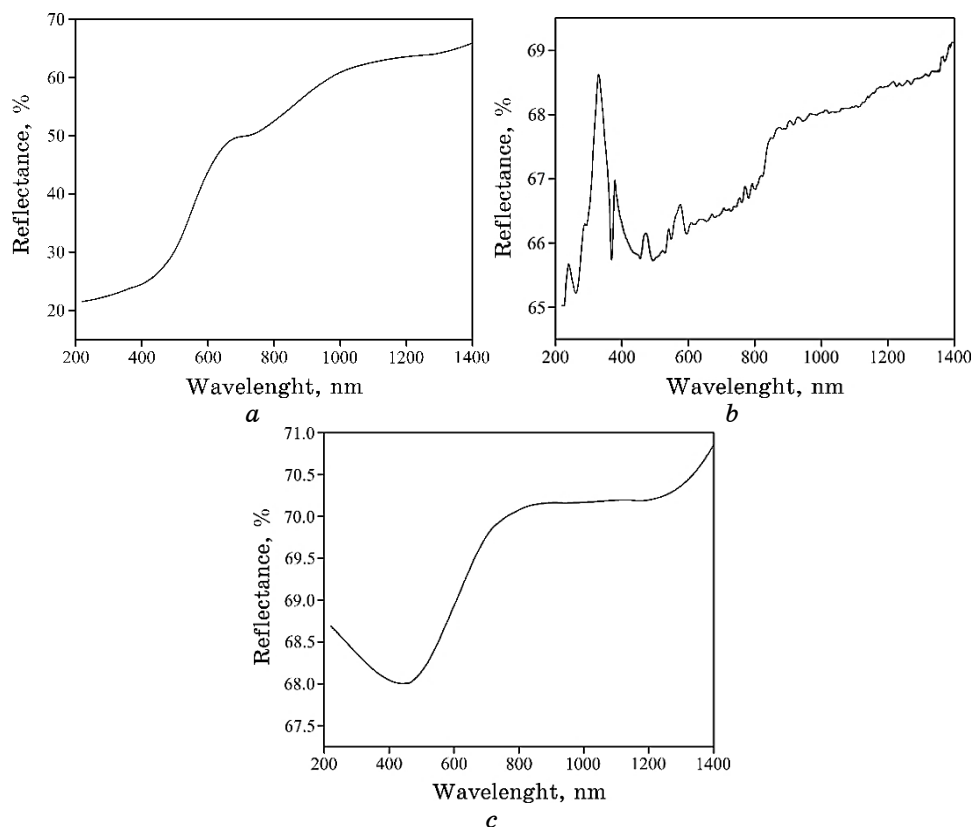


**Fig. 3.** UV-DRS reflectance spectrum of (a) Cu NPs, (b) Ag NPs, (c) Au NPs.

sample are taken into account. The resulting reflectance and absorbance spectra for Cu, Ag, Au NPs are presented in Figs. 3 and 4, respectively [13].

The unique optical properties of metal NPs can be attributed to their freely moving electrons. When excited by high-energy photons, these electrons induce surface-plasmon resonance, leading to strong absorption that is shape- and size-dependent [14].

The absorption spectra demonstrate that the synthesized metal NPs exhibit absorption across the entire visible region. Notably, silver NPs display a relatively narrow absorption band, particularly, in the visible range.

The cut-off wavelengths for Cu, Ag, and Au NPs are of 445 nm, 442 nm, and 435 nm, respectively.

This broad absorption is attributed to localized surface-plasmon resonance (LSPR), which enables the NPs to interact with a wide range of visible wavelengths. Consequently, noble metal NPs exhibit

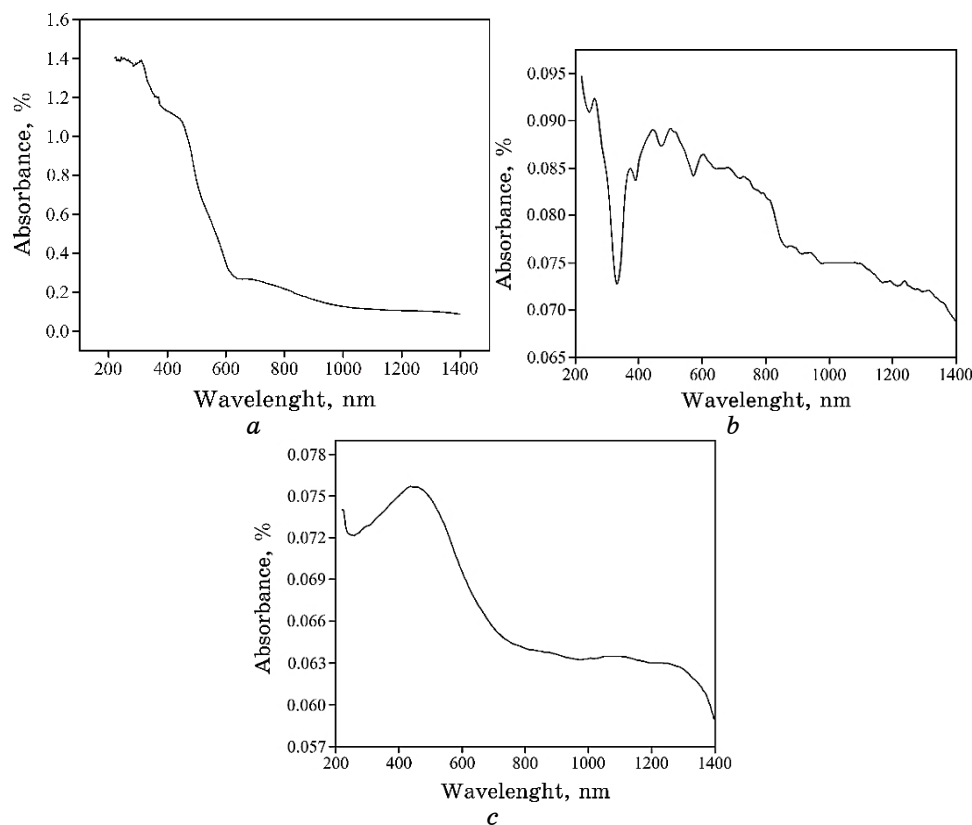


**Fig. 4.** UV-DRS absorption spectrum (a) Cu NPs, (b) Ag NPs, and (c) Au NPs.

maximum extinction at their plasmon-resonance frequency, occurring in the visible spectrum. This phenomenon underlies their potential applications in sensing technologies.

### 3.3. Band Gap Analysis

Noble metals possess high electron density, enabling them to absorb a broad spectrum of light and exhibit excellent reflectivity. Additionally, their lack of a band gap renders them as outstanding materials for exceptional electrical and thermal conductivity. Nevertheless, with their size in nanorange, they exhibit optical band gap as like semiconductors [15].

The band-gap energies of the synthesized NPs were determined using UV-DRS and analysed through Tauc plots based on the Kubelka–Munk theory [16]. The Tauc plots for Cu, Ag, and Au NPs are presented in Fig. 5, and the corresponding band-gap energies

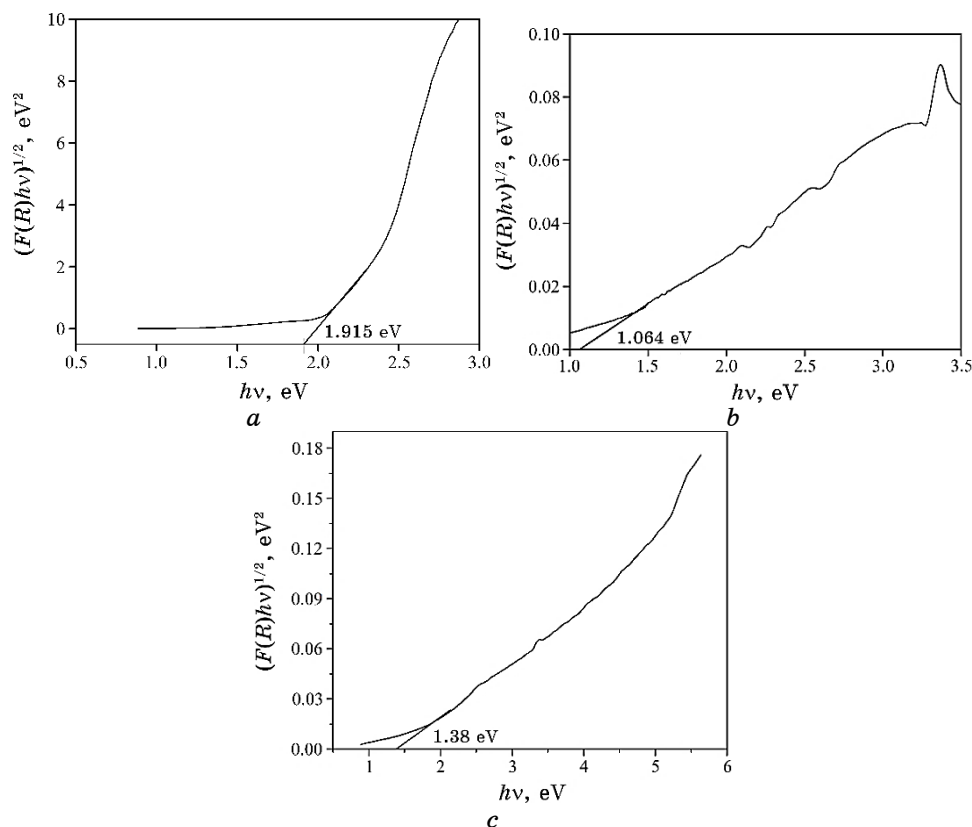


Fig. 5. Tauc plots for (a) Cu NPs, (b) Ag NPs, and (c) Au NPs.

TABLE 3. Optical parameters of prepared NPs.

No.	Metal	$E_g$ , eV	$n$	$R$	$\chi_e$	$\epsilon_r$
1	copper	1.92	2.8303	0.23	7.01	8.01
2	silver	1.06	3.0440	0.26	8.27	9.27
3	gold	1.38	3.4976	0.31	11.23	12.23

are summarized in Table 3.

Notably, the optical band-gap energies varied among the metals: silver exhibited the lowest value at 1.06 eV, while copper and gold had band-gap energies of 1.92 eV and 1.38 eV, respectively.

### 3.4. Determination of Optical Parameters

The established empirical correlation between the energy gap ( $E_g$ )

and refractive index ( $n$ ) facilitates the calculation of additional critical optical parameters, including reflectance ( $R$ ), dielectric constant ( $\epsilon_r$ ), and electric susceptibility ( $\chi_e$ ). The computed values for these parameters are presented in Table 3. Among copper, silver and gold, silver has the lowest band-gap energy and highest refractive index and dielectric constant [17].

Table 3 reveals that the synthesized NPs exhibit high refractive indices and dielectric constants, rendering them as ideal candidates for various photonic applications, including image sensors, anti-reflective coatings, electronic displays, and solar cells.

#### 4. CONCLUSIONS

The pure copper, silver and gold NPs are synthesized successfully by chemical reduction method. The prepared samples are in powder form. The powder x-ray diffraction analysis confirmed that the synthesized NPs are properly reduced to metallic nanopowder from its precursors. In addition, those are highly crystalline in nature belonging to the f.c.c. crystal lattice and perfectly matched with the reported studies. The UV-DRS analysis concludes that all the synthesized NPs have absorption in the entire visible region that confirms that the synthesized NPs possess LSPR property. Among Cu, Ag and Au NPs, Ag NPs have higher surface-plasmon resonance effect than the Cu and Au NPs. The solid form of noble-metal NPs enhanced the LSPR behaviour and making the metal NPs more promising for surface-plasmon resonance applications.

#### ACKNOWLEDGEMENTS

Mrs. R. Salome Mercy Ponrani (Register No. 21221282132005), Research Scholar, thankful to authorities of both Department of Physics, St. Xavier's College, Palayamkottai, Tirunelveli-627002, Tamilnadu, India (affiliated to Manonmanium Sundaranar University, Abishekapatti, Tirunelveli-627012, Tamilnadu, India) and Department of Physics, Sarah Tucker College, Tirunelveli-627007, Tamilnadu, India. The authors thank Heber Analytical Instrumentation Facility (HAIF), Trichy and Sophisticated Test and Instrumentation Facility (STIC), Cochin for taking characterization studies.

#### REFERENCES

1. Yachana Sharma and Pooja Kapoor, *Mater. Today Proc.*, **3**: 628 (2023); <https://doi.org/10.1016/j.matpr.2023.03.628>
2. A. M. Gaponov, O. L. Pavlenko, M. P. Kulish, O. P. Dmytrenko,

- A. I. Lesyuk, A. P. Onanko, N. V. Obernikhina, and V. B. Neimash, *Nanosistemi, Nanomateriali, Nanotehnologii*, **21**, Iss. 3: 495 (2023); <https://doi.org/10.15407/nnn.21.03.495>
3. Araa Hassan Hadi and Majeed Ali Habeeb, *Nanosistemi, Nanomateriali, Nanotehnologii*, **21**, Iss. 4: 779 (2023); <https://doi.org/10.15407/nnn.21.04.779>
  4. Yaoxin Fu, Tiegeng Liu, Haonan Wang, Ziyihui Wang, Lili Hou, Junfeng Jiang, and Tianhua Xu, *J. Sci.: Adv. Mater. Devices*, **9**, Iss. 2: 100694 (2024); <https://doi.org/10.1016/j.jsamd.2024.100694>
  5. Annalisa Scroccarello, Flavio Della Pelle, Michele Del Carlo, and Dario Compagnone, *Anal. Chim. Acta*, **1237**: 340594 (2023); <https://doi.org/10.1016/j.aca.2022.340594>
  6. M. P. Mcoyi, K. T. Mpofu, M. Sekhwama, and P. Mthunzi-Kufa, *Plasmonics*, **20**: 5481 (2025) (2024); <https://doi.org/10.1007/s11468-024-02620-x>
  7. Han-yue Deng, Liang Wang, Duo Tang, Yong Zhang, and Long Zhang, *Energetic Mater. Front.*, **2**, Iss. 3: 201 (2021); <https://doi.org/10.1016/j.enmf.2021.08.001>
  8. Md. Hazrat Ali, Md. Abul Kalam Azad, K. A. Khan, Md. Obaidur Rahman, Unesco Chakma, and Ajoy Kumer, *ACS Omega*, **8**, Iss. 31: 28133 (2023); <https://doi.org/10.1021/acsomega.3c01261>
  9. K. A. Madhushree, Poornima, R. Mahesh, Raviraj Kusanur, and H. G. Ashok Kumar, *Nanosistemi, Nanomateriali, Nanotehnologii*, **21**, Iss. 1: 0173 (2023); <https://doi.org/10.15407/nnn.21.01.173>
  10. Sumanveer Kaur, Ramneek Kaur, and Saurabh Gupta, *Phys. Scr.*, **99**, No. 11: 115993 (2024); <https://doi.org/10.1088/1402-4896/ad868a>
  11. M. I. Amrin, M. M. Roshan, R. Sai Gowri, and S. C. Vella Durai, *Semicond. Phys. Quantum Electron. Optoelectron.*, **27**, No. 2: 162(2024); <https://doi.org/10.15407/spqeo27.02.162>
  12. Stephan Link and Mostafa A. El-Sayed, *J. Phys. Chem. B*, **103**, No. 40: 8410 (1999); <https://doi.org/10.1021/jp9917648>
  13. K. Lance Kelly, Eduardo Coronado, Lin Lin Zhao, and George C. Schatz, *J. Phys. Chem. B*, **107**, No. 3: 668 (2003); <https://doi.org/10.1021/jp026731y>
  14. Sujit Kumar Ghosh and Tarasankar Pal, *Chem. Rev.*, **107**, Iss. 11: 4797 (2007); <https://doi.org/10.1021/cr0680282>
  15. Ibrahim Khan, Khalid Saeed, and Idrees Khan, *Arabian J. Chem.*, **12**, Iss. 7: 908 (2019); <https://doi.org/10.1016/j.arabjc.2017.05.011>
  16. Salmon Landi Jr., Iran Rocha Segundo, Elisabete Freitas, Mikhail Vasilevskiy, Joaquim Carneiro, and Carlos José Tavares, *Solid State Commun.*, **341**: 114573 (2022); <https://doi.org/10.1016/j.ssc.2021.114573>
  17. Osamu Wada, Doddoji Ramachari, Chan-Shan Yang, and Ci-Ling Pan, *J. Non-Cryst. Solids*, **573**: 121135 (2021); <https://doi.org/10.1016/j.jnoncrysol.2021.121135>